3D-hybrid mathematical model for analysis of abnormal neurological movements for the purposes of diagnosis and treatment of limb tremor

[1]Mykhaylo Bachynskyi[a], Mykhaylo Petryk[a], Vitaly Brevus[a] , Ivan Mudryk[a] , and Bohdan Glova[a]

[a] *Ternopil Ivan Puluj National Technical University, 56 Ruska str., Ternopil 46001, Ukraine*

Abstract

The suggested hybrid neural biosystem model provides an explanation for the condition and behavior of limb tremors by utilizing the propagation of wave signals. Specifically, it focuses on the segmental depiction of 3D trajectories of atypical neurological movements in the examined part of the body, while considering the matrix of cognitive influences from groups of neuroobjects in the central nervous system. Through the application of a hybrid integral transformation, which incorporates Fourier, Bessel, and Hilbert transforms, we have achieved a high-speed analytical solution to the model. This solution is presented in the form of a vector function that characterizes the 3D elements of trajectories during each segment of movement. Additionally, we introduce a methodology for calculating the hybrid spectral motion function, a system of orthogonal basic functions, and spectral values. These components form the foundation of the proposed hybrid transformation, offering integral vector solutions for the model. These solutions describe the elements of abnormal neurological movements trajectories and the distribution of absorbed components, taking into account feedback effects at both macro and micro levels.

Keywords

Tremor, abnormal movements, mathematical model, computer modeling, 3D-hybrid models, hybrid integral transforms, cognitive feedback signals

1. Introduction

The development of cutting-edge scientific models was driven by the collaborative efforts with French research institutions, including the University of Pierre and Marie Curie Sorbonne Paris 6, the Institute of Brain and Spinal Cord, and the Higher School of Industrial Physics and Chemistry in Paris. In this research, the authors have introduced innovative hybrid models to analyze the propagation of wave signals, aiming to understand the state and behavior of abnormal neurological movements (ANM) in specific body parts of a subject, referred to as T-objects. These movements are influenced by a particular group of neural nodes known as cerebral cortex (CC) neuro-objects.

These models are built on the foundation of integrated transforms and spectral analysis techniques tailored for various types of media. The research employs parallelization and component-wise assessment of interactions, resulting in explicit expressions for gradients of incoherent functionals. This approach facilitates the implementation of gradient methods for the identification of internal and external parameters.

The proposed hybrid model for neuro-biosystems provides a comprehensive description of the state and behavior of T-objects, focusing on the segmental depiction of 3D-trajectories associated with

[1]ITTAP'2023: 3nd International Workshop on Information Technologies: Theoretical and Applied Problems, November 22–24, 2023, Ternopil (Ukraine), Opole (Poland)

EMAIL: m.bachynskyi@gmail.com (A. 1); mykhaylo_petryk@tu.edu.te.ua (A. 2); v_brevus@tntu.edu.ua (A. 3); i1mudryk@ukr.net (A. 4); bogdanglova2014@gmail.com (A. 5)

ORCID: 0000-0001-6612-7213 (A. 1); 0000-0003-4139-7633 (A. 2); 0000-0002-7055-9905 (A. 3); 0000-0002-4305-1911 (A. 4); (A. 5).

abnormal neurological movements in a specific part (limb) of the T-object's body, taking neuro-objects into account. High-speed analytical solutions for the model, which describe trajectories for each neuromovement segment in vector form, are obtained using hybrid integral Fourier transformations. A novel method for calculating the hybrid spectral function of movement, a system of orthogonal basic functions, and spectral values form the basis of the proposed hybrid transformation, offering an integrated vector solution for the model.

2. A comprehensive approach and analytical instruments for diagnosing neurological conditions in T-objects utilizing the hybrid ANM model

These studies primarily emphasize the investigation of parameters pertaining to normal physiological conditions and behaviors, particularly the typical wave-like movements observed in specific body regions. To analyze these parameters, conventional digital processing techniques relying on integral Fourier transforms were employed. In prior works [2-3], cognitive feedback connections were roughly approximated through the utilization of methods and software technologies related to neural networks.

The methodology is founded on a hybrid model of the neuro-system, incorporating CC nodes and the tremor-object. This model was developed based on the theory of wave signal propagation and serves to delineate the states and behaviors of T-objects. It facilitates a segment-by-segment description of the 3D elements within the movements trajectories of the examined T-object, particularly focusing on the limbs of the hand. The model takes into consideration the matrix of cognitive influences emanating from groups of CC neuro-nodes on motion segments. These elements encompass the components of the hybrid spectral function across all signal segments. To dissect intricate ANM movements into more straightforward elements, the number of partitions can be flexibly selected, depending on the complexity of the ANM patterns. The mathematical model is designed to yield quantitative parameters related to tremors. An integral aspect of this method for analyzing the ANM data of a T-object is the remarkable capability to obtain a frequency response. This is achieved by applying a hybrid integral Fourier transform and employing digital signal processing techniques on hybrid spectral functions and spectral values [7, 8].

An electronic pen is employed for the recognition of handwritten content, including numbers, text, and template drawings, as well as for capturing and digitizing arbitrary movements of the hand. We have introduced a graphic digital pen device equipped with a built-in 3D microaccelerometer for conducting diagnostic assessments. The microcontroller is responsible for reading and processing data obtained from a three-axis acceleration sensor (microaccelerometer). In accordance with the proposed formulas, the system calculates the instantaneous coordinates of the accelerometer's position in space [8, 9]. Concurrently, data regarding the electronic pen's motion across the graphics tablet surface is collected.

Upon detecting zero pressure from the pen on the tablet's sensitive surface, signifying the pen's detachment from the surface, crucial information about the pen's movements is extracted from the microaccelerometer displays. This facilitates the determination of the instantaneous coordinates of the Micro-Electro-Mechanical Systems (MEMS) accelerometer's position in space, thereby ensuring the comprehensive acquisition of data pertaining to the trajectory of the ANM for the T-object and enhancing the data's reliability.

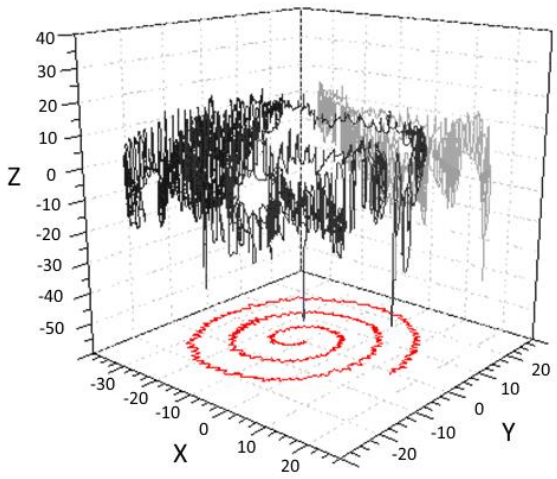

Figure 1: A 3D model of the ANM in the T-object, derived from data acquired via a microaccelerometer

The digitized pen position data is transmitted to the PC. This enhancement significantly bolsters the system's reliability in identifying the ANM of the T-object by integrating the tablet's sensitive element with an electronic pen and the embedded MEMS accelerometer.

The data pertaining to pen movements are utilized to generate a 3D model of the T-object's ANM, displayed in a graphical interface. This interface allows for the deconstruction of intricate 3D movements into three possible projections, enabling subsequent analysis of each projection. This analytical capability supports the selection of the most decisive parameters for ANM identification and comprehensive assessment [10].

3. The formulation and approach for the direct solution of inhomogeneous boundary value problems in the context of ANM analysis, considering the impact of cognitive feedback influences

As a result of this phenomenon, the patterns observed in electroencephalography (EEG) signals from neural nodes governing oscillatory neurological movements exhibit correlations. In essence, these correlations play a pivotal role in shaping the dynamics of the ANM for each segment of the track (referred to as the j-th segment), where n1 represents the number of division points for the abnormal neurological movements trajectories track (as depicted in Fig. 1). The division can be automatically configured in a flexible manner, accommodating any finite number of segments, each of which may possess varying lengths contingent upon the intricacy of the traffic areas and the selection of suitable basis functions. These basis functions are crucial for constructing acceptable dependencies for their approximation [13, 14]. Various criteria can be employed to determine the lengths of the partition elements, such as the amplitude characteristics of individual trends within the oscillating ANM trajectory [6, 7].

Mathematical Formulation of the Problem:

In accordance with the specified physical principles within the realm of neurological analysis, we can express the direct inhomogeneous initial-boundary value problem for ascertaining the parameters associated with the ANM of a T-object through a system of equations [6, 7].

$$\frac{\partial^2 u_{j_k}(t,x_k)}{\partial t^2} = b_{j_k}^2 \frac{\partial^2 u_{j_k}}{\partial x_k^{\,2}} + S_{j_k}^*(t,x_k), \quad x_k \in \left(l_{j_k-1}, l_{j_k}\right), j = \overline{1, n_1+1}, k = 1..3 \tag{1}$$

with initial conditions (homogeneous):

$$u_{j_k}(t,x_k)\Big|_{t=0} = 0, \qquad \frac{\partial u_{j_k}}{\partial t}\Big|_{t=0} = 0 \qquad , j_k = \overline{1, n_1+1}, k = 1..3, \tag{2}$$

Additionally, it involves homogeneous boundary conditions and a set of interface conditions:

$$\frac{\partial}{\partial x_k}u_1\left(t,x_k\right)_{x=0}=0,\quad \frac{\partial}{\partial z}u_n\left(t,x_k\right)_{x=l}=0, \tag{3}$$

$$\left[u_{j_k}\left(t,x_k\right)-u_{j_k}\left(t,x_k\right)\right]\Big|_{z=l_{j_k}}=0,k=1..3\left(b^2_{\ j_k}\frac{\partial}{\partial z}u_k\left(t,x_k\right)-b^2_{\ j_k+1}\frac{\partial}{\partial z}u_{j_k+1}\left(t,x_k\right)\right)\Big|_{z=l_{j_k}}=0,\ j_k=\overline{1,n_1},k=1..3 \tag{4}$$

in the multicomponent region $D^+_{n_1}=\left\{\left(t,x_k\right):t\in(0;\mathrm{T}),x_k\in I_{n_1}=\bigcup_{j_k=1}^{n_1+1}\left(l_{j_k-1},l_{j_k}\right);\ l_0=0,\ l_{n_1+1}\equiv l<\infty,k=1..3\right\}$.

Here (1.1) is a system of wave equations describing the ANM trajectories of tremor on each j-th segment of the trajectory $j_k=\overline{1,n_1+1},k=1..3$ depending on the resulting action of the set of signals $S^*_j\left(t,z\right)$, arriving from EEG-sensors for a certain set of KGM neural nodes that control the behavior of the studied T-object, b_{j_k}, $j_k=\overline{1,n_1+1},k=1..3$ - components of the phase velocity of propagation of the ANM waves, which are the amplitude characteristics of the wave tremor motion;

$S^*_{j_k}\left(\tau,\xi\right)=\sum_{i=1}^{n_2}\alpha_{j_ki}S_i\left(\tau,\xi\right),\ \left[\alpha_{j_ki}\right],\ j_k=\overline{1,n_1},\ i=\overline{1,n_2},k=1..3.$ - an adaptive matrix determines the connections and feedback-effects of specific KGM neuronodules on individual small segments of the ANR-track. The matrix element α_{j_ki} is a weighting coefficient (from 0 to 1), which determines the integral influence of the i-th neuronode S_i on the j_k -th segment of motion (determined by machine learning methods based on data mining [13]. The interface conditions (1.3), (1.4) ensure the continuity and integrity of the solution of the problem for the entire multicomponent domain of its definition.

Development of an analytical solution for the boundary value problem related to ANM. To establish an analytical solution for the direct inhomogeneous problem, denoted as (1) - (4), we employ the Hybrid Integral Fourier Transform (HIFT) as previously defined in [12]. This transformation relies on hybrid integral operators presented in matrix form.

- of direct action:

$$F_{n_1}\left[...\right]=\left[\int_{l_0}^{l_1}...V_1\left(x_k,\beta_m\right)\sigma_1dz\int_{l_1}^{l_2}...V_2\left(x_k,\beta_m\right)\sigma_2dx...\int_{l_{n_1-1}}^{l_{n_1}}...V_{n_1}\left(x_k,\beta_m\right)\sigma_{n_1}dz\int_{l_{n_1}}^{l_{n_1+1}}...V_{n_1+1}\left(x_k,\beta_m\right)\sigma_{n_1+1}dx\right], \tag{5}$$

- of reverse action:

$$F^{-1}_{n_1}\left[...\right]=\begin{bmatrix}\sum_{m=1}^{\infty}...V_1\left(x_k,\beta_m\right)\left(\left\|V\left(x_k,\beta_m\right)\right\|^2\right)^{-1}\\ \sum_{m=1}^{\infty}...V_2\left(x_k,\beta_m\right)\left(\left\|V\left(x_k,\beta_m\right)\right\|^2\right)^{-1}\\ .....\\ \sum_{m=1}^{\infty}...V_{n_1+1}\left(x_k,\beta_m\right)\left(\left\|V\left(x_k,\beta_m\right)\right\|^2\right)^{-1}\end{bmatrix}. \tag{6}$$

Here $\left[V_l\left(x_k,\beta_m\right)\right]_{,l=\overline{1,n_k+1}}$ - is the vector of the hybrid spectral function defined as follows:

$$\begin{bmatrix} V_1(x_k,\beta_m) \\ \dots \\ V_l(x_k,\beta_m) \\ \dots \\ V_{n_1+1}(z,\beta_m) \end{bmatrix} = \begin{bmatrix} \prod_{i=1}^{n_1} \xi_{i+1} \frac{\beta_m}{b_{i+1}} \left(\omega_0^2(\beta_m) \vartheta_1^{11}\left(\frac{\beta_m}{b_1} x_k\right) - \omega_0^1(\beta_m) \vartheta_1^{21}\left(\frac{\beta_m}{b_1} x_k\right)\right) \\ \dots \\ \prod_{i=l}^{n_1} \xi_{i+1} \frac{\beta_m}{b_{i+1}} \left(\omega_{l-1}^2(\beta_m) \vartheta_l^{11}\left(\frac{\beta_m}{b_k} x_k\right) - \omega_{l-1}^1(\beta_m) \vartheta_l^{21}\left(\frac{\beta_m}{b_k} x_k\right), \ _{l=\overline{2,n_1}}\right) \\ \dots \\ \omega_{n_1}^2(\beta_m) \vartheta_{n_1+1}^{11}\left(\frac{\beta_m}{b_{n_1+1}} x_k\right) - \omega_{n_1}^1(\beta_m) \vartheta_{n_1+1}^{21}\left(\frac{\beta_m}{b_{n_1+1}} x_k\right) \end{bmatrix}. \quad (7)$$

$\{\beta_m\}_{m=0}^{\infty}$ - the set of spectral values of the GIPF, which are the roots of the transcendental equation

$$\omega_{n_1}^2(\beta) \vartheta_{n+1}^{11}\left(\frac{\beta}{b_{n_1+1}} l_{n_1+1}\right) - \omega_{n_1}^1(\beta) \vartheta_{n_1+1}^{21}\left(\frac{\beta}{b_{n_1+1}} l_{n_1+1}\right) = 0. \quad (8)$$

It has been determined that the array of spectral values forms a monotonically ascending sequence that extends to positive infinity + ∞. Leveraging this observation, a recursive approach is introduced for computing the constituents of the hybrid spectral function of ANM. This methodology focuses on the identification of a set of orthogonal basic functions and serves as the foundation for the proposed hybrid transformation. The process ultimately results in an exhaustive vector solution pertinent to the theoretical mode:

$$\omega_{j_k}^i(\beta) = \omega_{j_k-1}^2(\beta) \psi_{i-1}^{j_k}\left(\frac{\beta}{b_{j_k}} l_{j_k}, \frac{\beta}{b_{j_k+1}} l_{j_k}\right) - \omega_{j_k-1}^1(\beta) \psi_{2i}^{j_k}\left(\frac{\beta}{b_{j_k}} l_{j_k}, \frac{\beta}{b_{j_k+1}} l_{j_k}\right)$$

$$\psi_{ij}^k\left(\frac{\beta}{b_k} l_k, \frac{\beta}{b_{k+1}} l_k\right) = \vartheta_{j_k}^{i1}\left(\frac{\beta}{b_{j_k}} l_{j_k}\right) \vartheta_{j_k}^{i2}\left(\frac{\beta}{b_{j_k+1}} l_{j_k}\right) - \vartheta_{j_k}^{i2}\left(\frac{\beta}{b_{j_k}} l_{j_k}\right) \vartheta_{j_k}^{i1}\left(\frac{\beta}{b_{j_k+1}} l_{j_k}\right), \quad i, = \overline{1,2}, \ j_k = \overline{1, n_1, k = 1..3}$$

$$\vartheta_{j_k}^{11}\left(\frac{\beta}{b_s} l_{j_k}\right) = \cos\left(\frac{\beta}{b_s} l_{j_k}\right), \ \vartheta_{j_k}^{21}\left(\frac{\beta}{b_s} l_{j_k}\right) = \sin\left(\frac{\beta}{b_s} l_{j_k}\right)$$

$$\vartheta_{j_k}^{12}\left(\frac{\beta}{b_s} l_{j_k}\right) = -\xi_s \frac{\beta}{b_s} \sin\left(\frac{\beta}{b_s} l_{j_k}\right), \quad \vartheta_{j_k}^{22}\left(\frac{\beta}{b_s} l_{j_k}\right) = \xi_s \frac{\beta}{b_s} \cos\left(\frac{\beta}{b_s} l_{j_k}\right), \ s \in \{l, l+1\}$$

$$\omega_k^1(\beta) = -\vartheta_k^{11}\left(\frac{\beta}{b_1} l_{0_k}\right), \quad \omega_{0_k}^2(\beta) = -\vartheta_{0_k}^{21}\left(\frac{\beta}{b_1} l_{0_k}\right).$$

$$\sigma_{j_k} = \frac{1}{b_{j_k}^2}, \ j = \overline{1, n_1}, k = \overline{1..3}.$$

Following this, we represent the system of equations (7) and the conditions (8) for the boundary value problem (1) - (4) using matrix notation:

$$\begin{bmatrix} \left(\frac{\partial^2}{\partial t^2} - b_1^2 \frac{\partial^2}{\partial x_k^{\ 2}}\right) u_1(t, x_k) \\ \left(\frac{\partial^2}{\partial t^2} - b_2^2 \frac{\partial^2}{\partial x_k^{\ 2}}\right) u_2(t, x_k) \\ \dots\dots\dots\dots\dots\dots\dots\dots\dots\dots\dots\dots\dots\dots\dots\dots\dots\dots\dots\dots \\ \left(\frac{\partial^2}{\partial t^2} - b_{n_1+1}^2 \frac{\partial^2}{\partial x_k^{\ 2}}\right) u_{n_1+1}(t, x_k) \end{bmatrix} = \begin{bmatrix} S_1(t, x_k) \\ S_2(t, x_k) \\ \dots\dots\dots\dots \\ S_{n_1+1}(t, x_k) \end{bmatrix}, \quad \begin{bmatrix} u_1(t, x_k) \\ u_2(t, x_k) \\ \dots\dots\dots\dots \\ u_{n_1+1}(t, x_k) \end{bmatrix}\Bigg|_{t=0} = 0, \quad \frac{\partial}{\partial t} \begin{bmatrix} u_1(t, x_k) \\ u_2(t, x_k) \\ \dots\dots\dots\dots \\ u_{n_1+1}(t, x_k) \end{bmatrix}\Bigg|_{t=0} = 0 \quad (9)$$

Applying to problem (9) the direct-action HIPF integral operator F_{n_1} (5), where $F_{n_1}\left[L_{n_1}\left[(x_k)\right]\right] = -\beta_m^2 u_m$ $L_{n_1}[...] = \sum_{j=1}^{n_1+1} b_j^2 \theta\left(x_k - l_{j-1}\right)\theta\left(l_j - x_k\right)\frac{d^2}{dx_k^2}$ - hybrid Fourier differential operator, θ - is the Heaviside step unit function, we obtain the Cauchy problem:

$$\left(\frac{d^2}{dt^2} + \beta_{m_k}^2\right)u_{m_k}(t) = S_{m_k}^*(t); \qquad u_{m_k}(t)\Big|_{t=0} = 0, \qquad \frac{d}{dt}u_{m_k}(t)\Big|_{t=0} = 0 \cdot$$

whose solution is the function [12, 13]:

$$u_{m_k}(t) = \int_0^t \frac{\sin\beta_{m_k}(t-\tau)}{\beta_{m_k}} S_{m_k}^*(\tau)\, d\tau \tag{10}$$

Applying to (10) the inverse integral GIPF operator $F_{n_1}^{-1}$ (6), after transformations, we obtain a unique solution to the homogeneous boundary value problem of ANM (1.1) - (1.4):

$$u_j(t, x_k) = \sum_{l=1}^{n_1+1}\int_0^t \int_{m_{k-1}}^{m_k} \mathcal{H}_{m_k k}(t-\tau, x_k, \xi) S_k^*(\tau, \xi)\sigma_k d\xi d\tau, \qquad j = \overline{1, n_1+1, k = 1..3}. \tag{11}$$

Here, the impact matrix is the response of the ANM system to the influence of the *k*-th segment of the resulting action of signals S_k^* a certain set of CC-neural nodes on the j-segment of the ANM track:

$$\mathcal{H}_{jk}(t, x_k, \xi) = \sum_{m_k=1}^{\infty} \frac{\sin\beta_{m_k} t}{\beta_{m_k}} \frac{V_j\left(x_k, \beta_{m_k}\right)V_l\left(\xi, \beta_{m_k}\right)}{\left\|V\left(z, \beta_{m_k}\right)\right\|^2}; \; j = \overline{1, n_1+1}, k = \overline{1..3}. \tag{12}$$

4. Identification of AMM amplitude components. Inverse inhomogeneous boundary value problem taking into account the cognitive feedback-influences of the neuro-nodes of the CC

Choice of residual functional. It is assumed that the amplitude components of the phase velocity of propagation of the ANM wave b_k, $k = \overline{1, n_1+1}$ boundary value problem (1) - (4) are unknown functions of time. However, on the surfaces of the regions $\gamma_k \subset \Omega_k$, $k = \overline{1, n_1+1}$, of an inhomogeneous medium, traces of solutions (trajectories of the ANR)

$$u_{l_k}(t, x_k)\Big|_{\gamma_k} = U_{l_k}(t, x_k)\Big|_{\gamma_k} \tag{13}$$

Thus, we have obtained problem (1) - (4), (13), which consists in finding the functions b_k, $l = \overline{1, n_1+1}, k = 1..3 \in D$, where $D = \left\{\nu(t,z):\ \nu|_{\Omega_{k_T}} \in C\left(\Omega_{k_T}\right),\ \nu > 0,\ l = \overline{1, n_1+1}, k = 1..3\right\}$.

The residual functional, which determines the deviation of the desired decoupling from the traces of the decoupling, obtained empirically on surfaces γ_k, can be written as follows:

$$J(b_k) = \frac{1}{2}\int_0^T \sum_{k=1}^{n+1}\left\|u_{s_k}(\tau, z, b_k) - U_k^*\right\|_{L_2(\gamma_k)}^2 \sigma_k\, d\tau \tag{14}$$

where $\|\varphi\|_{L_2(\gamma_k)}^2 = \int_{\gamma_k} \varphi^2 d\gamma_k$ – squared norm. In this case $\|\varphi\|_{L_2(\gamma_k)} = \left|\varphi(t,z)\right|_{z=\gamma_k}$.

The challenge of functionally identifying the amplitude parameters of ANM. The issue, as described in (1) - (4), requires a solution that involves implementing a procedure for the functional identification of the amplitude components of the phase velocity of ANM propagation. $b_k^2,\ k=\overline{1,n_1+1}$ as a function of time and conditions, known decoupling traces for each sufficiently thin k-th segment, $k=\overline{1,n_1+1}$, is transformed into a direct boundary value problem (15) - (17) as a system of homogeneous initial boundary value problems for successive thin segments of the ANR:

$$\frac{\partial^2}{\partial t^2}u_{l_k}\left(t,x_{l_k}\right)=b_{l_k}^2\frac{\partial^2}{\partial x_k^{\ 2}}u_{l_k}+S_{l_k}^{*}\left(t,x_k\right) \tag{15}$$

with initial conditions:

$$u_{l_k}\left(t,x_k\right)\Big|_{t=0}=0,\qquad \frac{\partial u_{l_k}}{\partial t}\Big|_{t=0}=0,\ l=\overline{1,n_1+1},k=1..3 \tag{16}$$

Boundary conditions on each of the thin segments of the ANM on *Z* coordinate*:*

$$u_{l-1}\left(t,x_k\right)\Big|_{x_k=L_{l_{k-1}}}=U_{L_{l_{k-1}}},\qquad u_{l_k}\left(t,x_k\right)\Big|_{x_k=L_{l_k}}=U_{\ l_k},\ l=\overline{1,n_1+1},k=1..3 \tag{17}$$

Choice of residual functional. It is assumed that the components of the phase velocity of propagation of the ANM wave b , $k=\overline{1,n_1+1}$ of the boundary value problem (15) - (17) are unknown functions of time. With known values of the pen position $u_k(t,z)$ at observation points on segments of the ANM $\gamma_k\subset\Omega_k,\ k=\overline{1,n_1+1}$:

$$u_{\ l_k}\left(t,x_k\right)\Big|_{\gamma_{l_k}}=U_{L_{l_k}}\left(t,x_k\right)\Big|_{\gamma_{l_k}} \tag{18}$$

the initial-boundary value problem (15) - (17) can be considered for each point *z* for each thin k_1-th segment of the ANM trace and will consist in finding the functions $b_k\in D$, where $D=\left\{\nu(t,z):\ \nu\big|_{\Omega_{k_1T}}\in C\left(\Omega_{k_1T}\right),\ \nu>0,\ k=\overline{1,n_1+1}\right\}$.

The residual functional of the deviation of the solution from its traces on $\gamma_{k_1}\in\Omega_{k_1}$, and can be obtained as follows

$$J_{l_k}\left(b_{l_k k}\right)=\frac{1}{2}\int_0^T\left(\left\|u_{l_k}\left(t,x_k,b_{l_k}\right)-U_{l_k}^{*}\right\|^2\right)dt \tag{19}$$

Approach for addressing the direct boundary value identification problem. The process of constructing and providing mathematical support for the problem's solution is achieved through the application of the finite integral Fourier transform [12, 13]. By utilizing integral operators [10], we apply them to the problem outlined in (15) - (17)::

$$F\left[u_{l_k}\left(t,x_k\right)\right]=\int_{l_k-1}^{L_{l_k}}u_{l_k}\left(t,x_k\right)V_m\left(\beta_m,x_k\right)dx_k\equiv U_{l_k m}(t)\ ,$$

$$F^{-1}\left[U_{l_k m}\left(t\right)\right]=\sum_{m=0}^{\infty}U_{l_k\,\mathrm{m}}\left(t\right)\frac{V_m\left(\beta_m,x_k\right)}{\left\|V_m\left(\beta_m,x_k\right)\right\|^2}\equiv u_{l_k}\left(t,x_k\right)\ , \tag{20}$$

$$F\left[\frac{\partial^2}{\partial^2 z}u_k\left(t,x_k\right)\right]=-\beta_m^2U_{l_k m}(t)+\beta_m U_{L_{l_{k-1}}}\left[1-(-1)^m\frac{U_{L_{l_k}}}{U_{L_{l_{k-1}}}}\right]=-\beta_m^2U_{l_k m}(t)+\beta_m U_{L_{l_{k-1}}}-\beta_m(-1)^m U_{L_{l_k}}\ ,$$

$$V_m(\beta_m, x_k) = \sin\beta_m\left(x_{l_k} - L_{l_k-1}\right),\ \beta_m = \frac{m\pi}{\Delta h},\ \|V_m\|^2 = \int_{l_{k-1}}^{l_k}\left[V_m(\beta_m, x_k)\right]^2 dx_k = \frac{\Delta l}{2},$$

the Cauchy problem is obtained:

$$\frac{d^2}{dt^2}U_{km}(t, x_k) = -b_k^2\beta_m^2 U_{km}(t) + b_k^2\beta_m U_{l_{k-1}}\left[1-(-1)^m\frac{U_{l_k}}{U_{l_{k-1}}}\right] + S_{km}^*(t) \tag{21}$$

$$u_{l_k m}(t, x_k)\big|_{t=0} = 0,\ \left.\frac{\partial u_{l_k m}}{\partial t}\right|_{t=0} = 0, l_k = \overline{1, n_1+1}, k = 1..3 \tag{22}$$

The unique solution to the Cauchy problem (1.21), (1.22) has the form:

$$U_{l_k m}(t) = \int_0^t \frac{\sin b_{l_k}\beta_m(t-\tau)}{b_{l_k}\beta_m}\left[S_{l_k m}^*(\tau) + b_{l_k}^2\beta_m\left(U_{L_{l_{k-1}}} - (-1)^m U_{L_{l_k}}\right)\right]d\tau \tag{23}$$

Passing to the originals in (23), we obtain a unique solution to the original boundary value problem (15) - (17) in the classical form.

$$u_{l_k}(t, x_k) = \int_0^t\int_{L_{l_k-1}}^{L_{l_k}}\mathcal{H}_{l_k}^1(t-\tau, x_k, \xi)S_{l_k}^*(\tau, \xi)\,d\xi d\tau + \int_0^t\left(\mathcal{H}_{l_k}^{21}(t-\tau, x_k, L_{l_k-1})U_{l_{k-1}} - \mathcal{H}_{l_k}^{22}(t-\tau, x_k, L_{l_k})U_{L_{l_k}}\right)d\tau\,. \tag{24}$$

Here, the components of the influence vectors have the form:

$$\mathcal{H}_k^1(t-\tau, x_k, \xi) = \frac{2}{\Delta h}\sum_{m=0}^{\infty}\frac{\sin b_k\beta_m(t-\tau)}{b_k\beta_m}\sin\beta_m(\xi - l_{k-1})\sin\beta_m(x_k - l_{k-1})$$

$$\mathcal{H}_k^{21}(t, x_k, l_{k-1}) = \frac{2b_k}{\Delta h}\sum_{m=0}^{\infty}\sin b_k\beta_m t\sin\beta_m(x_k - l_{k-1}) \tag{25}$$

$$\mathcal{H}_k^{22}(t, x_k, L_{x_k}) = \frac{2b_{l_k}}{\Delta h}\sum_{m=0}^{\infty}\sin\left(b_{l_k}\beta_m t\right)(-1)^m\sin\beta_m\left(x_k - L_{l_k-1}\right)\,.$$

The solution (24) to the problem described in (15) - (17) undergoes a sequence of transformations, leading it to a format that is both convenient and efficient for numerical iterative computations and for application in parameter identification procedures. By integrating, substituting explicit expressions for influence functions, and conducting several transformations, the equations (25) are simplified into straightforward algebraic expressions that are highly suitable for the identification process. This eliminates the necessity for iterations in this phase of the regularization identification process, markedly enhancing the overall efficiency. Thus, after integration, we arrive at the following result:

$$S_{l_k}^*\int_0^t\int_{L_{l_k-1}}^{L_{l_k}}\mathcal{H}_k^1(t-\tau, x_k, \xi)d\xi d\tau = \frac{2}{\Delta h}S_{l_k}^*\sum_{m=\dot{a}}^{\infty}\frac{1-\cos\left(b_{l_k}\beta_m t\right)}{\left(b_{l_k}\beta_m\right)^2}\frac{1}{\beta_m}\left((-1)^m - 1\right)\sin\beta_m\left(x_k - L_{l_k-1}\right)$$

$$U_{l_{k-1}}\int_0^t\mathcal{H}_k^{21}(t, x_k, l_{k-1})d\tau = U_{l_{k-1}}\frac{2}{\Delta h}\sum_{m=0}^{\infty}\frac{1-\cos\left(b_k\beta_m t\right)}{\beta_m}\sin\beta_m(x_k - l_{k-1}) \tag{26}$$

$$U_{l_k}\int_0^t\mathcal{H}_k^{22}(t, x_k, l_{k-1})d\tau = U_{l_k}\frac{2}{\Delta h}\sum_{m=0}^{\infty}(-1)^m\frac{1-\cos\left(b_k\beta_m t\right)}{\beta_m}\sin\beta_m(x_k - l_{k-1})$$

After substituting expressions (26) into (24), we finally obtain:

$$u_k(t,z)=\frac{2}{\Delta h}\sum_{m=0}^{\infty}\frac{1-\cos\left(b_k\beta_m t\right)}{\beta_m}\sin\beta_m\left(x_k-l_{k-1}\right)\left(S_k^*\frac{1}{\left(b_k\beta_m\right)^2}\left(\left(-1\right)^m-1\right)+U_{l_{k-1}}\left(1-\left(-1\right)^m\frac{U_{l_k}}{U_{l_{k-1}}}\right)\right) \quad (27)$$

Formulas for the gradient components. We derive analytical expressions for the gradient components of the residual functional:

$$\nabla J_{\tilde{b}_k}=\int_0^T\int_{l_{k-1}}^{l_k}\phi_k(t,x_k)\frac{\partial^2}{\partial z^2}u_k(t,x_k)dx_k dt \quad . \quad (28)$$

In the context of the functional identification problem, we derive the subsequent formulas for the gradient components of the residual functional:

$$\nabla J_{\tilde{b}_k}\left(t\right)=\int_{l_{k-1}}^{l_k}\phi_k(t,x_k)\frac{\partial^2}{\partial {x_k}^2}u_k(t,x_k)dx_k \quad , \quad (29)$$

$$\phi_k\left(t,x_k\right)=\frac{2}{\Delta h}\sum_{m=0}^{\infty}\frac{1-\operatorname{ch}\left(b_k\beta_m\left(T-t\right)\right)}{\left(b_k\beta_m\right)^2}\sin\beta_m\gamma_k\sin\beta_m\left(x_k-l_{k-1}\right)\left(U_k^*-u_{k_k}^n\right),\ l=\overline{1,n_1+1},k-1..3$$

$$u_k\left(t,x_k\right)=\frac{2}{\Delta h}\sum_{m=0}^{\infty}\frac{1-\cos\left(b_k\beta_m t\right)}{\beta_m}\sin\beta_m\left(x_k-l_{k-1}\right)\left(S_k^*\frac{1}{\left(b_k\beta_m\right)^2}\left(\left(-1\right)^m-1\right)+U_{l_{k-1}}\left(1-\left(-1\right)^m\frac{U_{l_k}}{U_{l_{k-1}}}\right)\right)$$

$$\frac{\partial^2}{\partial z^2}u_k\left(t,x_k\right)=-\frac{2}{\Delta h}\sum_{m=0}^{\infty}\beta_m\left(1-\cos\left(b_k\beta_m t\right)\right)\sin\beta_m\left(x_k-l_{k-1}\right)\left(S_k^*\frac{1}{\left(b_k\beta_m\right)^2}\left(\left(-1\right)^m-1\right)+U_{l_{k-1}}\left(1-\left(-1\right)^m\frac{U_{l_k}}{U_{l_{k-1}}}\right)\right)$$

Regularization expressions for the n+1 -th step of defining the identifying functional dependency. Using the method of minimum errors to determine the dependence of the identification of the amplitude components of the phase velocity of propagation of the ANM-wave $\tilde{b}^{n+1}_{l_k}$ on time for each l_k - th element of the ANM $l_k=\overline{1,n_1+1},k=1..3$, we obtain

$$\tilde{b}_{l_k}^{n+1}\left(t\right)=\tilde{b}_{l_k}^{n}\left(t\right)-\nabla J_{b_{l_k}}^{n}\left(t\right)\frac{\left\|u_{l_k}^n\left(t,\gamma_{l_k},\tilde{b}_{l_k}^n\right)-U_{l_k}^*\right\|^2}{\left\|\nabla J_{b_{l_k}}^{n}\left(t\right)\right\|_{\gamma_{l_k}}^2},\ t\in\left(0,T\right),\ l_k=\overline{1,n_1},k=1..3 \quad (30)$$

A valuable and efficient approach to scrutinize the acquired outcomes is through cyclic computations, wherein the analyzed data sets are progressively reduced in proportion. In essence, estimates are derived and compared at each iteration of the analyzed data constraints. These results, illustrated in the form of frequency and amplitude characteristics, serve as the fundamental components for assessing a patient's condition via computerized diagnostic methods. Integral aspects of this development encompass algorithms for obtaining simulated system parameters, the capability to visually represent the obtained outcomes, and the necessity for dynamically adjusting system parameters.

These factors collectively enhance the presentation of results, providing greater clarity, and promoting the focused utilization of the technology. A successful feature of this advancement is its deployment as an autonomous module, functioning as a library that permits the continuous enhancement of methods and the sustainability of research relevance.

5. Displaying the digital analysis of the patient's movement trajectory

As illustrated in Fig. 2, these movements exhibit significant heterogeneity, featuring numerous segments with pronounced high-amplitude and high-frequency abnormal movements. To enhance the visualization of the trajectory graph for the ANM of the T-object, as depicted in Fig. 1, it is presented in a temporal-spatial format. In this format, the sections of the oscillating abnormal movement trajectories become clearly discernible, revealing their dependence on time and their remarkable variation within short time intervals (Fig. 2).

To conduct a more detailed examination of these ANM movement segments, they can be subdivided according to specific time intervals under study. This allows for the investigation of their real amplitude and frequency characteristics concerning the integral time distributions of cognitive signals from the CC nodes.

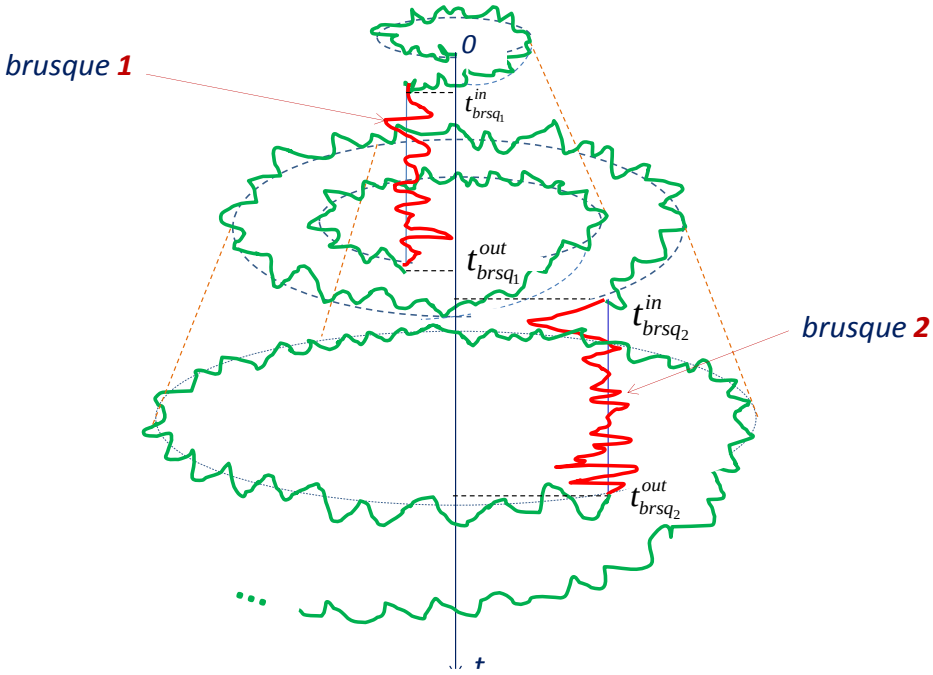

Figure 2: Temporal-spatial representation of the ANM in the T-object, highlighting specific segments characterized by intense vibrational abnormal movements that vary with time within short intervals.

6. Conclusions

We have developed a hybrid model of a neuro-bio-system that elucidates the state and behavior of the 3D elements within the trajectories of abnormal movements in T-objects. This model takes into consideration the matrix of cognitive influences originating from groups of neuro-nodes in the cerebral cortex. Utilizing the techniques of hybrid integral Fourier transforms, we propose high-performance algorithms for the identification of parameters in the studied feedback systems. These algorithms enable component-wise estimation of mutual influences by explicit expressions for the gradients of the residual functional, facilitating parallel computations on multi-core computers.

In contrast to the conventional classical approach, our proposed hybrid model prioritizes a deep decomposition of the system while preserving its integrity and essential connections. This approach allows for a more comprehensive description of the complex underlying mechanisms, especially those involving numerous internal connections and cognitive feedback influences. It enhances data completeness, which was previously overlooked during conventional statistical processing.

The software implementation in this manner enhances adaptability and ease of integration into diverse systems for research purposes. Mathematical methods, specifically their calculation algorithms, have been translated into a set of classes with associated methods that emulate their functionality. Software modules, classes, and their interactions have been consolidated into a unified library module, fostering the versatile use of the input data analysis method across various practical applications and

programs.By incorporating the 3D microaccelerometer module within the digital pen of a graphics tablet, we maintain the existing high measurement accuracy while additionally gaining the capability to monitor the separation of the pen from the surface along the Xz-axes.

7. References

[1] A.N. Khimich, M.R. Petryk, D.N. Mykhalyk, I.V. Boyko, A.V. Popov, V.A. Sydoruk, Methods for mathematical modeling and identification of complex processes and systems based on visoproductive computing (neuro- and nanoporous cyber-physical systems with feedback, models with sparse structure data, parallel computing). Monograph, Kiev: National Academy of Sciences of Ukraine. Glushkov Institute of Cybernetics. 2019. - 176 p. ISBN: 978-966-02-9188-1.

[2] Petryk, M., Pastukh, O., Bachynskiy, M., Mudryk, I., Stefanyshyn, V. Processing of Cerebral Cortex Neurosignals from EEG Sensors and Recognizing Specific Types of Mechanical Movements Elements of Pacient Limbs under the Cognitive Feedback Influenses. CEUR Workshop Proceedingsthis link is disabled, 2023, 3468, pp. 61–70

[3] R. Bhidayasiri, Z. Mari, Digital phenotyping in Parkinson's disease: Empowering neurologists for measurement-based care. Parkinsonism Relat Disord. 2020 Nov; 80:35-40. DOI: 10.1016/j.parkreldis.2020.08.038.

[4] V. Rajaraman, D. Jack, S.V. Adamovich, W. Hening, J. Sage, H. Poizner, A novel quantitative method for 3D measurement of Parkinsonian tremor. Clinical neurophysiology, 11(2), 187-369 (2000)

[5] D. Haubenberger, D. Kalowitz, F.B. Nahab, C. Toro, D. Ippolito, D.A. Luckenbaugh, L. Wittevrongel, M. Hallett, Validation of Digital Spiral Analysis as Outcome Parameter for Clinical Trials in Essential Tremor. Movement Disorders 26 (11), 2073-2080, (2011)

[6] E.D. Louis, A. Gillman, S. Böschung, C.W. Hess, Q. Yu, & S.L. Pullman, High width variability during spiral drawing: Further evidence of cerebellar dysfunction in essential tremor. Cerebellum, 11, 872-879 (2012).

[7] P. Viviani, P.R. Burkhard, S.C. Chiuvé, C.C. dell'Acqua, P. Vindras, Velocity control in Parkinson's disease: a quantitative analysis of isochrony in scribbling movements. Exp Brain 2009; 194:259–83.

[8] G. LO, A.R. Suresh, L. Stocco, S. González-Valenzuela, and V. C. Leung, "A wireless sensor system for motion analysis of Parkinson's disease patients," (PERCOM Workshops), 2011 IEEE International Conference on. IEEE, pp. 372-375, 2011

[9] Bhidayasiri R., Mari Z. Digital phenotyping in Parkinson's disease: Empowering neurologists for measurement-based care. Parkinsonism Relat Disord. 2020 Nov;80:35-40. DOI: 10.1016/j.parkreldis.2020.08.038.

[10] Grimaldi G., Manto M. Neurological tremor: sensors, signal processing & emerging applications. Sensors. 2010;10(2):1399–1422. DOI: 10.3390/s100201399.

[11] Mykhaylo Petryk, Tomasz Gancarczyk, Oleksander Khimich (2021) Methods mathematical modeling and identification of complex processes and systems on the basis of high-performance calculations (neuro- and nanoporous feedback cyber systems, models with sparse structure data, parallel computations), Akademia Techniczno-Humanistyczna w Bielsku-Białej, Bielsko-Biała, p.195.

[12] Mudryk I., Petryk M.. High-performance modeling, identification and analysis of heterogeneous abnormal neurological movement's parameters based on cognitive neuro feedback-influences. Innovative Solutions in Modern Science. 2021. New York. TK Meganom LLC. V1(45). P. 235-249 doi: 10.26886/2414-634X.1(45)2021.16.

[13] Glova B., Mudryk I. Application of Deep Learning in Neuromarketing Studies of the Effects of Unconscious Reactions on Consumer Behavior. 2020 IEEE Third International Conference on Data Stream Mining & Processing (DSMP): Conference, Lviv, 21-25 August 2020. P. 337–340. DOI: 10.1109/DSMP47368.2020.9204192